Online user-friendly slant total electron content computation from IRI-Plas: IRI-Plas-STEC

Hakan Tuna[1], Orhan Arikan[1], Feza Arikan[2], Tamara L. Gulyaeva[3], and Umut Sezen[2]

[1]Department of Electrical and Electronics Engineering, Bilkent University, Ankara, Turkey, [2]Department of Electrical and Electronics Engineering, Hacettepe University, Ankara, Turkey, [3]IZMIRAN, Moscow, Russia

Abstract Slant total electron content (STEC), the total number of free electrons on a ray path, is an important space weather observable. STEC is the main input for computerized ionospheric tomography (CIT). STEC can be estimated using the dual-frequency GPS receivers. GPS-STEC contains the space weather variability, yet the estimates are prone to measurement and instrument errors that are not related to the physical structure of the ionosphere. International Reference Ionosphere Extended to Plasmasphere (IRI-Plas) is the international standard climatic model of ionosphere and plasmasphere, providing vertical electron density profiles for a desired date, time, and location. IRI-Plas is used as the background model in CIT. Computation of STEC from IRI-Plas is a tedious task for researchers due to extensive geodetic calculations and IRI-Plas runs. In this study, IONOLAB group introduces a new space weather service to facilitate the computation of STEC from IRI-Plas (IRI-Plas-STEC) at www.ionolab.org. The IRI-Plas-STEC can be computed online for a desired location, date, hour, elevation, and azimuth angle. The user-friendly interface also provides means for computation of IRI-STEC for a desired location and date to indicate the variability in hour of the day, elevation, or azimuth angles. The desired location can be chosen as a GPS receiver in International GNSS Service (IGS) or EUREF Permanent Network (EPN). Also instead of specifying elevation and azimuth angles, the user can directly choose from the GPS satellites and obtain IRI-Plas-STEC for a desired date and/or hour. The computed IRI-Plas-STEC values are presented directly on the screen or via e-mail as both text and plots.

1. Introduction

The ionosphere is a layer in the atmosphere which lies in the altitudes ranging from about 90 km to 1000 km. Ionosphere is distinguished from other layers of the atmosphere because it is ionized mainly by solar radiation. It has crucial importance in satellite communication because of its conductive, inhomogeneous, anisotropic, temporally and spatially varying, and temporally and spatially dispersive nature.

The most important parameter for modeling the ionosphere is the electron density profile which is a direct way to investigate the structure and variability of the ionosphere as well as the ionospheric influence on radio waves. Radio waves are reflected and/or refracted as they travel through ionosphere based on the electron density distribution in the layers of the ionosphere.

Total electron content (TEC) is defined as the line integral of electron density on a given ray path. TEC corresponds to the total number of free electrons in a cylindrical path with a 1 m^2 cross-sectional area, and it is widely used in space weather studies for investigation of ionospheric variability. The unit of TEC is TECU where 1 TECU is equal to 10^{16} electrons/m^2. When TEC is calculated on a vertical path in the local zenith direction, it is called vertical total electron content (VTEC). Slant TEC (STEC) is usually used to designate the total number of electrons on a ray path other than the local zenith direction.

Ionosphere is the main source of error for Global Navigation Satellite Systems (GNSS) due to its highly variable structure, and it causes unpredictable time delays. Without calculating the ionospheric delay and inserting it into their measurement models, GNSS systems can not obtain high-resolution position estimates. The widely used Global Positioning System (GPS) provides a cost-effective means for computation of STEC (GPS-STEC) using pseudorange and phase delay recordings of dual-frequency Earth-based receivers [*Komjathy*, 1997; *Schaer*, 1999; *Davies and Hartmann*, 1997; *Arikan et al.*, 2003]. GPS-STEC is used both in correction of positioning errors due to ionospheric delays and also in ionospheric physics to capture the underlying structure of ionosphere using computerized ionospheric tomography such as in *Erturk et al.* [2009], *Sibanda* [2010], *Jin and Jin* [2011], and *Hirooka et al.* [2012]. The GPS-STEC measurement model

includes instrumental biases that need to be determined to increase the positioning resolution and reduce nonionospheric components from STEC. Unfortunately, due to ambiguities and uncertainties, GPS-STEC can never be obtained in such a way to represent ionospheric and plasmaspheric part alone [*Komjathy*, 1997; *Schaer*, 1999; *Arikan et al.*, 2008].

There are approaches in the literature for calculation of STEC values by using an ionosphere model. Generally, thin-shell approximation is adopted and STEC values are related to the VTEC values with an obliquity factor [*Lanyi and Roth*, 1988; *Manucci et al.*, 1998; *Mushini et al.*, 2009]. Thin-shell method is an oversimplified approximation method that ignores the inhomogeneous structure of the ionosphere. In order to take into account the variation of electron density along the ray path, line integration methods are generally used such as in *Cabrera et al.* [2005] and *Nava et al.* [2008]. In *Cabrera et al.* [2005], the electron density profile along the slant path is obtained from International Reference Ionosphere (IRI) [*Bilitza*, 2001] and Chapman models with 20 km segments, and integrated electron density values are computed between 50 km and 2000 km. In *Nava et al.* [2008], a method for fast computation of STEC values is introduced where electron density values are obtained from NeQuick2 model, which is an updated version of the NeQuick ionosphere model [*Radicella*, 2009]. The numerical STEC computation based on NeQuick2 is provided as an online tool available at "http://t-ict4d.ictp.it/nequick2/nequick-2-web-model." On the website, STEC path can be defined by latitude, longitude, and height. The lower end can also be obtained using the cursor position and online map, and higher end can be defined using the satellite position in azimuth, elevation, and height. Year, month, and time are the temporal variables. Solar activity can be provided by the user, or it can be chosen from recorded values. The STEC values are computed using the model electron density values in *Nava et al.* [2008], and the output is provided in a text file on-screen, providing the electron density along the ray path. The electron density profile is also plotted in a graph in jpeg format. The major drawback of IRI and NeQuick electron density profiles is the modeling of topside ionosphere and plasmasphere [*Coïsson et al.*, 2006].

In order to overcome the modeling difficulties of electron density in plasmasphere, IRI model is recently modified into International Reference Ionosphere extended to Plasmasphere (IRI-Plas) to extend the height coverage to GPS satellite altitude of 20,200 km [*Gulyaeva*, 2010]. In IRI-Plas, the electron density values are obtained by an updated-scale parameter set [*Gulyaeva et al.*, 2011; *Gulyaeva*, 2012]. IRI-Plas model gives greater proximity to real measurement values [*Maltseva et al.*, 2013; *Gulyaeva et al.*, 2013] and is recently designated as the international standard model for ionosphere and plasmasphere [*Gulyaeva and Bilitza*, 2012].

In this study, a new IONOLAB online user-friendly STEC calculation tool is introduced at www.ionolab.org website. This unique IONOLAB service utilizes IRI-Plas model and line integration method for STEC calculation and presents a web-based service with comprehensive features. The ionosphere and plasmasphere are divided into horizontal layers by using preset altitude step sizes. Small altitude step sizes are used for high electron density regions, and larger altitude step sizes are used for low electron density regions. The altitude values extend from 100 km to 20,000 km, which covers the plasmasphere and the ionosphere. For a given slant path, the spherical coordinates of the points where the slant path reaches the mean altitude of these layers and the length of the slant path within the corresponding layers are calculated. The electron density values at the calculated locations on the propagation path are obtained from IRI-Plas model for the default climatic ionospheric parameters, which would provide us the climatic component of STEC. Electron content contribution at each layer is calculated by multiplying the electron density values and the length of the propagation path within the corresponding layer. Finally, STEC values are calculated as the summation of these electron density contributions. By changing the input parameters and repeating the same procedure, variation of STEC with respect to hour, satellite elevation angle, and satellite azimuth angle can be generated.

In IRI-Plas-STEC web service, the electron density values along the chosen ray path can be obtained for a desired location, date, hour, elevation, and azimuth angle. The computed STEC value is provided as a number in TECU. The electron density profile values along the ray path are also given in a text file on-screen. The variation of STEC with respect to hour in a day, elevation angle, and azimuth angle can also be observed for a desired location and date. Since these options require multiple STEC calculations, computation time increases. Therefore, when they are ready, computed results are sent to the user via user-defined e-mail address as an attachment. In the attachment, both the computed STEC values and its graphical
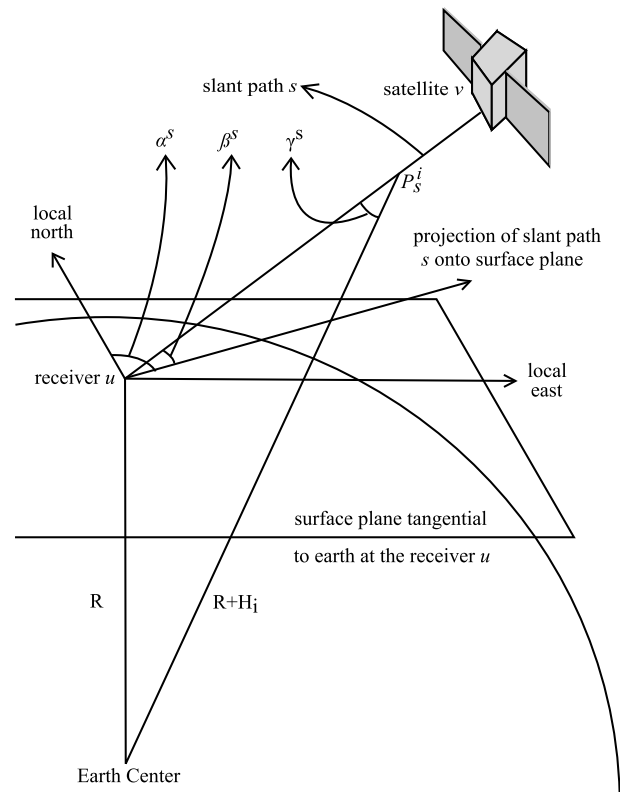
Figure 1. Slant path geometry and STEC calculation parameters.

representation are given. In the future, to obtain near-real-time results, it is planned to provide an option of performing STEC computation by using coarser discretization of the line integrals. In order to facilitate the comparison of model-based IRI-Plas-STEC with measurement-based GPS-STEC values, the desired location can be chosen from International GNSS Service (IGS) stations [*International GNSS Service*, 2013] or EUREF Permanent Network (EPN) stations [*EUREF*, 2013] using the four-digit GPS station codes or selecting from the provided IGS station map. Also to define the upper end of the STEC ray path, any desired GPS satellite can be chosen online through the Pseudorandom noise (PRN) identification numbers. For the chosen GPS satellite, either a STEC value for the given hour is computed or the value of STEC on the satellite path is computed for the given day and provided in a plot. These unique computational capabilities enable users from various disciplines to observe model-based variability of STEC in time, elevation, and azimuth.

In section 2, proposed STEC calculation method from IRI-Plas model is explained. In section 3, STEC calculation service is presented.

2. STEC Calculation From IRI-Plas

In this section, the mathematical details of STEC computation are provided. The parameter s indicates the slant path along which STEC to be computed as given in Figure 1. In order to calculate the STEC along a given slant path s, the coordinates of the points on the slant path s and the electron density values at the corresponding locations from IRI-Plas model are required.

A slant path s can be uniquely defined as the propagation path between receiver u and satellite v, for a given time t. The coordinates of the slant path s and the slope of the slant path s are calculated for discrete height values contained in array $\underline{H}$ in increasing order. In the following calculations, H_i represents the ith height level in array $\underline{H}$ and P_i^s represents the point where slant line s reaches height H_i. The Earth is considered as a sphere with a radius of 6378 km, which will be denoted as R. Before beginning calculations, suppose that, the parameters listed in Table 1 are given as input parameters.

Let γ_i^s represent the angle between the slant path s and the surface normal, which intersects s at point P_i^s, and let D_i^s represent the distance between the receiver u and the point P_i^s. By using the law of sines and law

Table 1. Input Parameters for Calculating the Slant Path Coordinates

Symbol	Definition
$\phi(u)$	Latitude of Receiver u
$\lambda(u)$	Longitude of Receiver u
α^s	Satellite Elevation Angle
	The angle between the surface plane at the receiver u location and the slant path s
β^s	Satellite Azimuth Angle
	The clockwise angle between the local north vector at the receiver u location and the projection of the slant path s onto the surface plane which is tangential to Earth at the receiver u location

of cosines, γ_i^s and D_i^s can be calculated as follows:

$$\gamma_i^s = \sin^{-1}\left(\frac{R}{R+H_i}\sin\left(\frac{\pi}{2}+\alpha^s\right)\right), \tag{1}$$

$$D_i^s = \sqrt{R^2 + \left(R+H_i\right)^2 - 2R\left(R+H_i\right)\cos\left(\frac{\pi}{2}-\alpha^s-\gamma_i^s\right)}. \tag{2}$$

After D_i^s is calculated, the local east, north, up (ENU) coordinates of the point P_i^s can be calculated by using (3).

$$\begin{bmatrix} E(P_i^s) \\ N(P_i^s) \\ U(P_i^s) \end{bmatrix} = \begin{bmatrix} D_i^s \cos(\alpha^s)\cos\left(\frac{\pi}{2}-\beta^s\right) \\ D_i^s \cos(\alpha^s)\sin\left(\frac{\pi}{2}-\beta^s\right) \\ D_i^s \sin(\alpha^s) \end{bmatrix}, \tag{3}$$

where $E(P_i^s)$, $N(P_i^s)$, and $U(P_i^s)$ represent the local east, north, and up coordinates of point P_i^s, respectively, in ENU coordinate system. These ENU coordinates are transformed to Earth Centered Earth Fixed (ECEF) coordinates by using (4), (5), and (6).

$$\underline{\underline{T}}^u = \begin{bmatrix} -\sin(\lambda(u)) & \sin(\phi(u))\cos(\lambda(u)) & \cos(\phi(u))\cos(\lambda(u)) \\ -\cos(\lambda(u)) & \sin(\phi(u))\sin(\lambda(u)) & \cos(\phi(u))\sin(\lambda(u)) \\ 0 & \cos(\phi(u)) & \sin(\phi(u)) \end{bmatrix}, \tag{4}$$

$$\begin{bmatrix} X(u) \\ Y(u) \\ Z(u) \end{bmatrix} = \begin{bmatrix} R\cos(\phi(u))\cos(\lambda(u)) \\ R\cos(\phi(u))\sin(\lambda(u)) \\ R\sin(\phi(u)) \end{bmatrix}, \tag{5}$$

$$\begin{bmatrix} X(P_i^s) \\ Y(P_i^s) \\ Z(P_i^s) \end{bmatrix} = \underline{\underline{T}}^u \begin{bmatrix} E(P_i^s) \\ N(P_i^s) \\ U(P_i^s) \end{bmatrix} + \begin{bmatrix} X(u) \\ Y(u) \\ Z(u) \end{bmatrix}. \tag{6}$$

In equations (4), (5), and (6), $\underline{\underline{T}}^u$ represents the transformation matrix; $X(u)$, $Y(u)$, and $Z(u)$ represent the x, y, z coordinates of receiver u; $X(P_i^s)$, $Y(P_i^s)$, and $Z(P_i^s)$ represent the x, y, z coordinates of point P_i^s, respectively, all in ECEF coordinate system.

After the ECEF coordinates of point P_i^s are obtained, spherical latitude (ϕ) and spherical longitude (λ) of P_i^s, which will be used as inputs to IRI-Plas, are calculated as follows:

$$\phi(P_i^s) = \frac{180}{\pi}\tan^{-1}\left(\frac{Z(P_i^s)}{\sqrt{(X(P_i^s)^2 + Y(P_i^s)^2)}}\right), \tag{7}$$

$$\lambda(P_i^s) = \frac{180}{\pi}\tan^{-1}\left(\frac{Y(P_i^s)}{X(P_i^s)}\right). \tag{8}$$

Note that for unambiguous determination of $\phi(P_i^s)$ and $\lambda(P_i^s)$, inverse tangent functions shall be used together with the quadrant information.
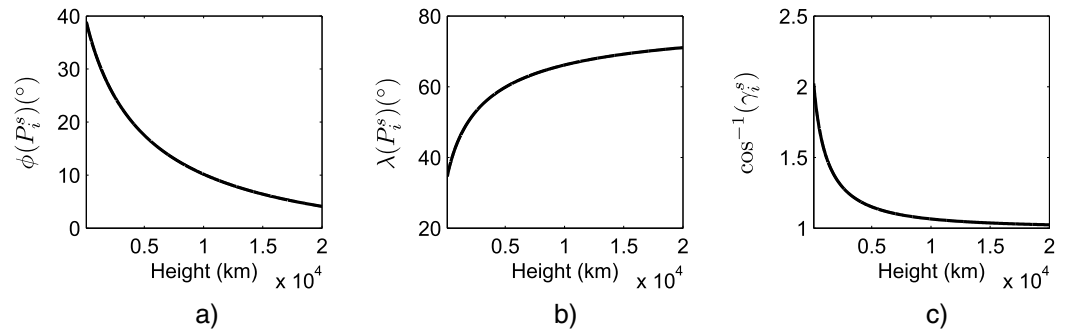
Figure 2. (a) $\phi(P_i^s)$, (b) $\lambda(P_i^s)$, and (c) $\cos^{-1}(\gamma_i^s)$ with respect to elevation for input parameters $\phi(u) = 39.92°$, $\lambda(u) = 32.85°$, $\alpha^s = 28°$, and $\beta^s = 126°$.

Suppose that ΔH_i is the height step value used at height H_i. In order to find the electron density contribution at each height, the length of the slant path s within the height step ΔH_i, which will be denoted as ΔH_i^s, should be calculated. For this purpose, the following trigonometric relation can be used:

$$\Delta H_i^s = \frac{\Delta H_i}{\cos(\gamma_i^s)}. \tag{9}$$

Finally, IRI-Plas model-based STEC value along the slant path s, which will be denoted as $STEC^s$, can be approximated by integrating the electron density contributions from each height along the slant path s as nonuniform Riemann sum:

$$STEC^s = \sum_{i=1}^{I} Ne(\phi(P_i^s), \lambda(P_i^s), H_i)\Delta H_i^s, \tag{10}$$

where $Ne(\phi(P_i^s), \lambda(P_i^s), H_i)$ represents the electron density value obtained from IRI-Plas model for given latitude $\phi(P_i^s)$, longitude $\lambda(P_i^s)$, and height H_i, and I is the length of array $\underline{H}$. For illustrative purposes, Figure 2 shows the $\phi(P_i^s)$, $\lambda(P_i^s)$, and $\cos^{-1}(\gamma_i^s)$ dependence to the height, respectively, for a sample STEC calculation for the set of input parameters $\phi(u) = 39.92°$, $\lambda(u) = 32.85°$, $\alpha^s = 28°$, and $\beta^s = 126°$.

In choosing the set of layers whose heights are denoted with vector $\underline{H}$, the trade-off between the accuracy and efficiency of the computation is considered. A longer vector $\underline{H}$ with denser height levels will yield more precise results while increasing the computational time. A nonuniform separation of layers with denser height levels at higher electron density regions and sparse height levels at lower electron density regions provides acceptable results.
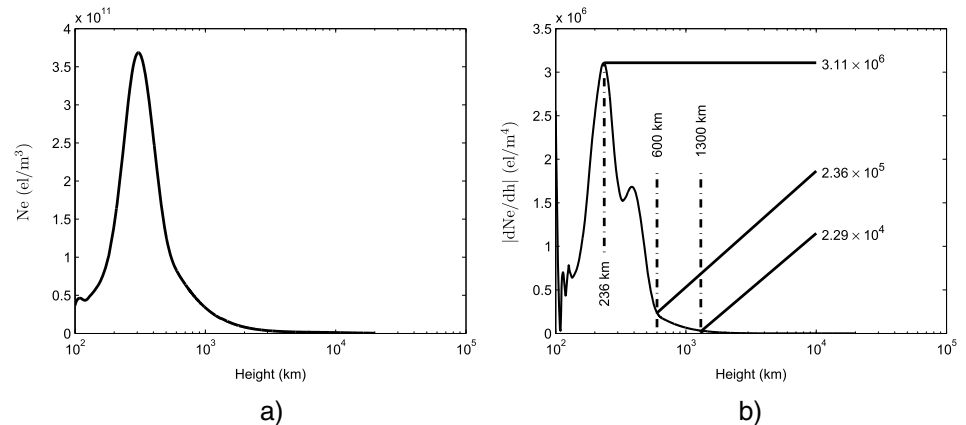

Figure 3. (a) Mean value of 1000 randomly generated vertical electron density profiles from IRI-Plas, for randomly selected positions on Earth, for randomly selected dates between 1 January 2003 and 1 January 2013, and for random hours. (b) Mean value of the absolute values of the first-order derivatives of 1000 randomly generated vertical electron density profiles used in Figure 3a, with respect to height.
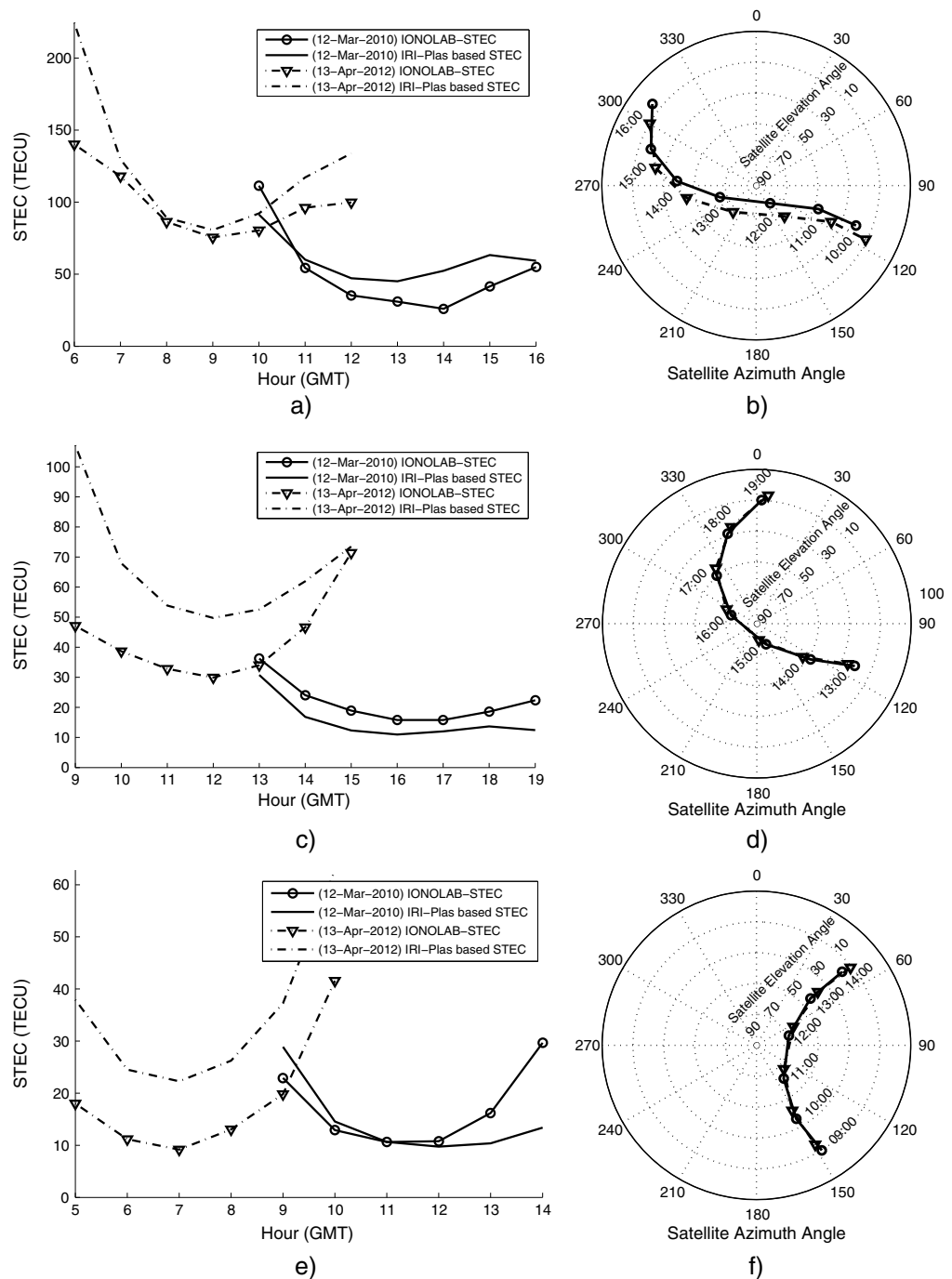
Figure 4. Comparison of IRI-Plas-STEC and IONOLAB-STEC values with respect to hour for 12 March 2010 (quiet day) and 13 April 2012 (geomagnetically disturbed day): (a) ntus, PRN 16; (c) ankr, PRN 7; and (e) kir0, PRN 20. Satellite tracks in local polar coordinate system for (b) PRN 16, (d) PRN 7, and (f) PRN 20.

In order to investigate the proper selection of H, 1000 different vertical electron density distribution functions are generated by using IRI-Plas, for randomly selected positions on Earth and for randomly selected dates between 1 January 2003 and 1 January 2013 and for random hours of the day. Figure 3a shows the mean value of the obtained electron density distributions, and Figure 3b shows the mean value of the absolute values of the first-order derivatives of the obtained electron density distributions, with respect to height. The regions with higher first-order derivative require denser allocation of the layers. The maximum value of the first-order derivative is reached at the height of 236 km. At a height of 600 km, this value drops below 8% of the maximum value. At 1300 km height and above, IRI-Plas model employs plasmasphere
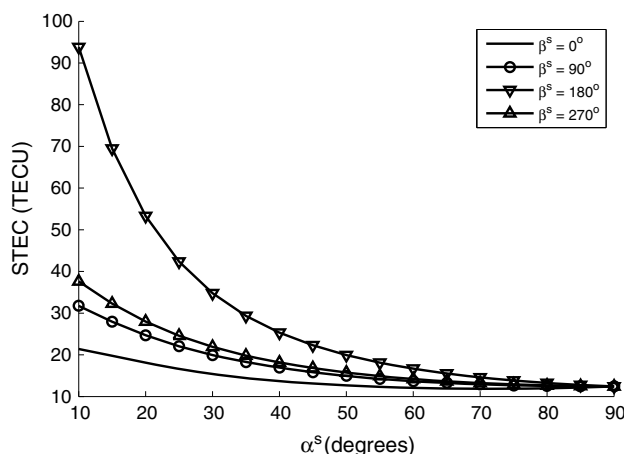
Figure 5. IRI-Plas-based STEC calculations with respect to satellite elevation angle parameter on 22 April 2009 at 12:00 GMT for a receiver station located at coordinates (39°N, 35°E) and for a GPS satellite position located at north, east, west, and south of the receiver station.

equations, and the first-order derivative drops below 0.8% of its maximum value. Consequently, use of 1 km height step sizes between 100 and 600 km, 10 km step sizes between 600 and 1300 km, and 50 km step sizes between 1300 and 20,000 km has been found to provide acceptable computational results.

2.1. STEC With Respect to Hour of the Day

By using the proposed methodology, real STEC measurements obtained from GPS systems can be directly compared with the IRI-Plas model-based STEC estimates. For this purpose, IONOLAB-STEC data is used as experimental GPS measurement [*Nayir et al.*, 2007]. Figure 4 shows a comparison of IRI-Plas-STEC calculations and GPS-based STEC measurements (IONOLAB-STEC data) with respect to hour. Two different days are selected for calculations: 12 March 2010, which is a quiet day, and 13 April 2012, which is a geomagnetically disturbed day. IONOLAB-STEC and IRI-Plas-STEC values are computed for three different GPS receiver stations located at equatorial, mid and high latitude regions. The equatorial station "ntus" is located at Singapore, Republic of Singapore, the mid latitude station "ankr" is located at Ankara, Turkey, and the high latitude station 'kir0' is located at Kiruna, Sweden. Receiver location and satellite angles for each hour, which are required to calculate IRI-Plas-STEC values, are obtained from IONOLAB-STEC computations. For each station, a satellite that passes close to local zenith angle is chosen. These satellites are PRN 16 for ntus, PRN 7 for ankr and PRN 20 for kir0. Figure 4 indicates that the computations of STEC from IRI-Plas and IONOLAB-STEC are in agreement with each other for a quiet day, yet they may differ significantly on a geomagnetically disturbed day. This is mainly due to the fact that IRI-Plas Ne profiles are based on Consultative Committee on International Radio (CCIR) monthly median coefficients.

2.2. STEC With Respect to Satellite Elevation Angle

In order to see the effect of satellite elevation angle in the STEC estimation, STEC values are calculated for synthetic satellite positions which have constant satellite azimuth angles and a range of satellite elevation angles in the interval [10°, 90°] with a step size of 10°. Figure 5 shows STEC values obtained on 22 April 2009, 12:00 Greenwich Mean Time (GMT), for a receiver station located at coordinates (39°N, 35°E). Four different satellite azimuth angles are used in calculations: 0° (north), 90° (east), 180° (south), and 270° (west). Note that STEC values converge to the same vertical TEC value as the satellite elevation angle increases. As the satellite elevation decrease, STEC estimates show variation based on the electron density distribution at the corresponding azimuth directions. Figure 5 indicates higher electron density values in the south and lower electron density values in the north. Typically, in GPS measurements, ionosphere is considered to be uniform and homogeneus for satellite elevation angles greater than 60°. Calculating STEC values by sweeping a range of satellite elevation angles provides a means to investigate the validity of this commonly used assumption.

2.3. STEC With Respect to Satellite Azimuth Angle

Investigation of STEC with respect to satellite azimuth angles provide characteristics of anisotropy in the ionosphere. For this purpose, STEC values are calculated for synthetic satellite positions which have constant satellite elevation angles and a range of satellite azimuth angles in the interval [0°, 350°] with a step size
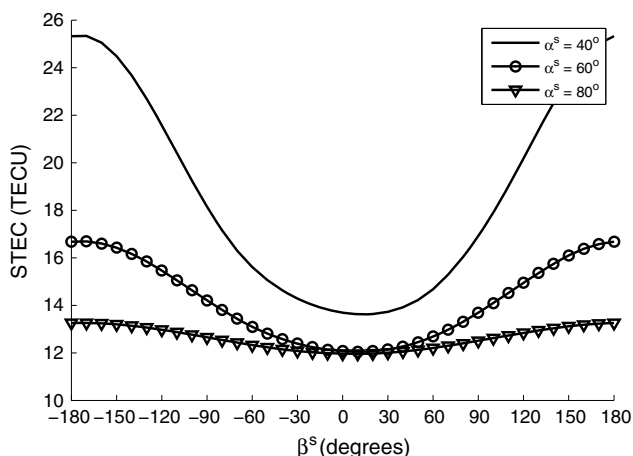
Figure 6. IRI-Plas-based STEC calculations with respect to satellite azimuth angle parameter on 22 April 2009 at 12:00 GMT for a receiver station located at coordinates (39°N, 35°E) and for satellite elevation angles of 40°, 60°, and 80°.

of 10°. Figure 6 shows STEC values obtained on 22 April 2009, 12:00 GMT, for a receiver station located at coordinates (39°N, 35°E). Three different satellite elevation angles are used in calculations: 40°, 60°, and 80°. The calculated STEC is minimum for azimuth angle of 10° and maximum for azimuth angle of −170°, which indicates an increase in the electron density toward the south. Figure 6 also indicates the effect of satellite elevation angle on the STEC measurements. As the satellite elevation angle decreases, the effect of satellite azimuth angle on the STEC measurements gets stronger. This functionality also demonstrates the validity of azimuthal homogeneity assumptions with respect to satellite elevation angles.

3. Online STEC Calculation Service

In order to present an online, easy-to-use STEC calculation service, proposed STEC estimation approach is implemented as a public web-based service at www.ionolab.org. Users have to register to the website before using the IRI-Plas-STEC service. In order to use this service, users do not need to download any program or program code; all calculations are performed online by the IONOLAB service. For a given time, satellite, and receiver parameters, STEC values are calculated and presented to user online or via e-mail. For receiver parameters, user can input receiver coordinates or four-character IGS or EPN station code. For satellite parameters, user can input satellite elevation angle and azimuth angle values or just the GPS satellite number. IRI-Plas-STEC service is a unique application which accepts IGS or EPN station codes and GPS satellite numbers as slant path input parameters. This property simplifies the model-based estimations of STEC corresponding to real STEC measurement scenarios. Furthermore, optional services for calculating STEC by sweeping hour of the day, satellite elevation angle, and satellite azimuth angle parameters are also integrated to this service. Figure 7 shows a screenshot of the IRI-Plas-STEC service.
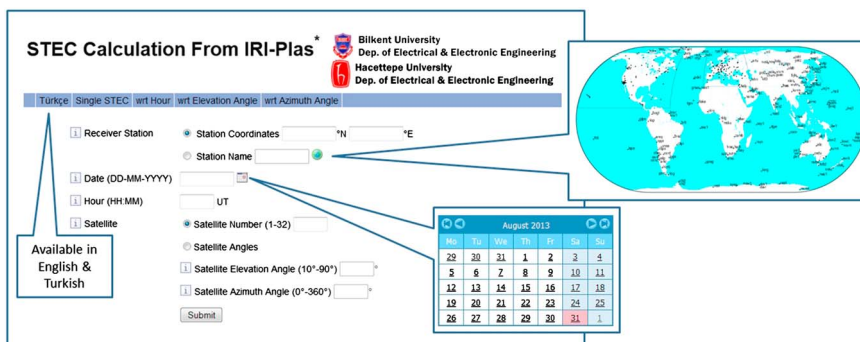

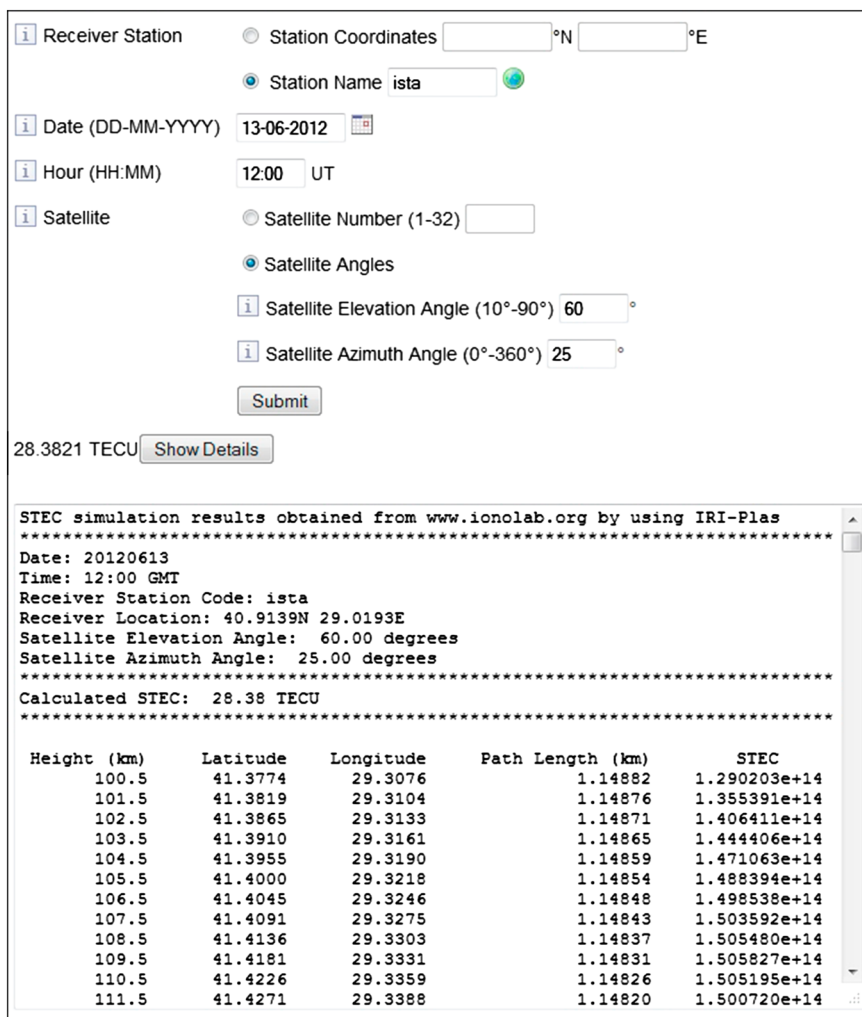**Figure 7.** Screenshot of online IRI-Plas-STEC service main page at www.ionolab.org.

Figure 8. Screenshot of the computed single IRI-Plas-STEC value.

3.1. Single STEC Calculation

Single STEC calculation option is the default functionality provided by the IRI-Plas-STEC service. This option calculates a single STEC value for a given time, receiver, and satellite parameters. For receiver parameters, user can choose between specifying the coordinates of the receiver or entering the four-digit IGS or EPN station code. For satellite parameters, user can input satellite angles or a GPS satellite number. IONOLAB service collects information about the given receiver and satellites or uses given coordinate and angle parameters directly to calculate the requested STEC value. Results are presented to the user online, together with calculation details such as slant path parameters and electron density values on the slant path obtained from IRI-Plas. Calculation time for a single STEC takes a couple of minutes. Figure 8 shows the screenshot of a sample single STEC calculation results. In this example, receiver station is selected as "ista," which is located in Istanbul, Turkey; calculation date is selected as 13 June 2012, 12:00 GMT; satellite elevation angle is selected as 60°; and the satellite azimuth angle is selected as 25° yielding an estimated result of 28.31 TECU. Calculation details such as the coordinates of the receiver station, coordinates of the slant path as the altitude reaches definite altitude values and the electron density values at these points, and the length of the slant path at each altitude step are also provided to the user.

3.2. STEC Calculation With Respect to Hour of the Day

In this option, user provides date, receiver, and satellite parameters in order to obtain hourly IRI-Plas-STEC values at a specified date. If the user specifies satellite angles, IRI-Plas-STEC values are calculated hourly for corresponding fixed slant path. However, if the user specifies the GPS satellite number, GPS satellite positions on the given date are obtained from satellite ephemerides data, and IRI-Plas-STEC values are
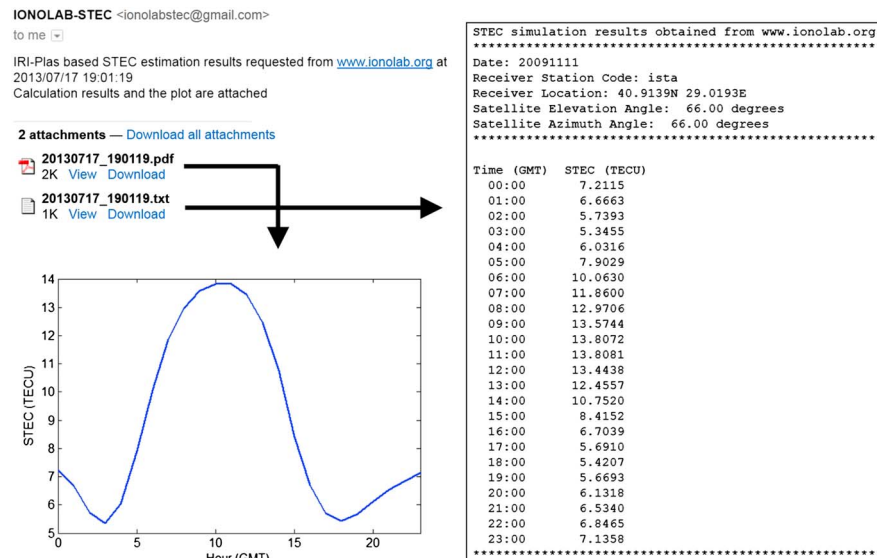
Figure 9. Screenshot of an e-mail sent by IRI-Plas-STEC service that contains requested STEC calculation results with respect to hour.

calculated hourly for a slant path that follows the satellite. Calculation time for this option takes about an hour; therefore, every calculation request is queued at the server, and when the calculations are completed, user is informed by an e-mail together with the detailed results and a plot of the obtained results. If the user enters the four-digit IGS or EPN station code and GPS satellite number, this option provides a very informative tool for the comparison of GPS-based daily STEC measurements and IRI-Plas-based STEC estimates. Figure 9 shows a sample e-mail providing the obtained results. In this example, receiver station is selected as "ista," which is located in Istanbul, Turkey. The calculation date is selected as 11 November 2009; satellite elevation angle and satellite azimuth angle are selected as 66°. IRI-Plas-STEC service automatically retrieves coordinates of the receiver station and calculates STEC values from 00:00 GMT to 23:00 GMT with hourly intervals on the specified date. Figure 9 shows that the calculated STEC values change between 5.34 TECU, which is obtained at 03:00 GMT, and 13.08 TECU, which is obtained at 11:00 GMT.
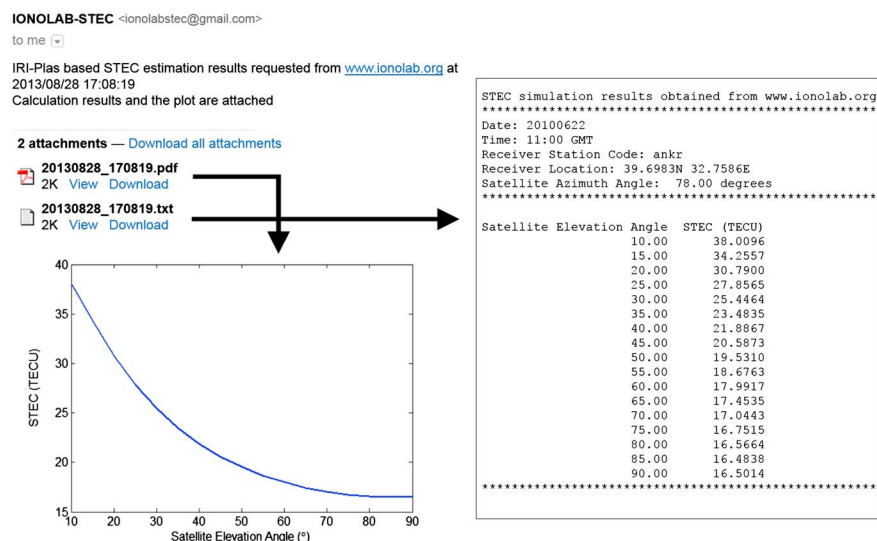

Figure 10. Screenshot of an e-mail sent by IRI-Plas-STEC service that contains requested STEC calculation results with respect to satellite elevation angle.
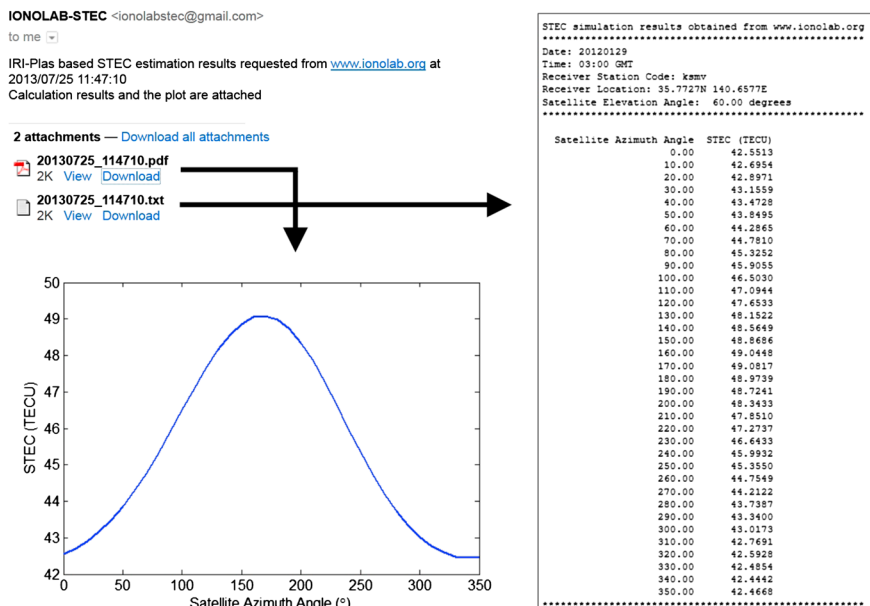
Figure 11. Screenshot of an e-mail sent by IRI-Plas-STEC service that contains requested STEC calculation results with respect to satellite azimuth angle.

3.3. STEC Calculation With Respect to Satellite Elevation Angle

In this option, user provides date, receiver, and satellite azimuth angle parameters. User can specify the coordinates of the receiver or enter the four-digit IGS or EPN station code. STEC values are calculated for satellite elevation angle values between 10° and 90° with a step size of 10°. Calculation time for this option is about half an hour, which also depends on the overall calculation load on the IONOLAB server. Therefore, every calculation request is queued at the server, and when the calculations are finished, user is informed by an e-mail together with the detailed results and a plot. Figure 10 shows content of a sample e-mail. In this example, receiver station is selected as "ankr," which is located in Ankara, Turkey. The calculation time is selected as 22 June 2010, 11:00 GMT, and the satellite azimuth angle is selected as 78°. IRI-Plas-STEC service automatically retrieved coordinates of the receiver station and calculated STEC values for satellite elevation angle values ranging from 10° to 90° with a step size of 10°. Figure 10 shows that the calculated STEC values have a range between 16.48 TECU, which is obtained for 85° satellite elevation angle, and 38 TECU, which is obtained for 10° satellite elevation angle.

3.4. STEC Calculation With Respect to Satellite Azimuth Angle

In this option, user specifies date, receiver, and satellite elevation angles. User can specify the coordinates of the receiver or enter the four-digit IGS or EPN station code. STEC values are calculated for satellite azimuth angle values between 0° and 350° with a step size of 10°. Calculation time for this option is about an hour; therefore every calculation request is queued at the server, and when the calculations are finished, user is informed by an e-mail together with the detailed results and a plot. This option provides valuable information for analyzing the anisotropic characteristics of the ionosphere. Figure 11 shows content of a sample e-mail. In this example, receiver station is selected as "ksmv," which is located in Kashima, Japan. The calculation date is specified as 29 January 2009, 03:00 GMT, and the satellite elevation angle is selected as 60°. IRI-Plas-STEC service automatically retrieved coordinates of the receiver station and calculated STEC values for satellite azimuth angle values ranging from 0° to 350° with a step size of 10°. Figure 11 shows that the calculated STEC values have a range between 42.44 TECU, which is obtained for 340° satellite azimuth angle, and 49.08 TECU, which is obtained for 170° satellite azimuth angle.

4. Conclusions

An efficient computational technique is proposed for the estimation of STEC from a given 3-D model of the ionosphere. IRI-Plas model, which is an extended version of IRI to the plasmasphere is used for the estimation of the climatic component of the 3-D electron density profile in the ionosphere. Proposed method

approximates required line integration with a nonuniform Riemann sum for precise calculation of STEC values from IRI-Plas model. A user-friendly web service based on the presented IRI-Plas-STEC calculation approach has been implemented at www.ionolab.org website, together with the calculation options such as STEC with respect to satellite elevation angle, satellite azimuth angle, and hour of the day parameters. The IRI-Plas-STEC values can be used in various studies for ionospheric research and recovery of GNSS ionospheric delay errors.

References

Arikan, F., C. B. Erol, and O. Arikan (2003), Regularized estimation of vertical total electron content from Global Positioning System data, *J. Geophys. Res.*, *108*(A12), 1469, doi:10.1029/2002JA009605.

Arikan, F., H. Nayir, U. Sezen, and O. Arikan (2008), Estimation of single station interfrequency receiver bias using GPS-TEC, *Radio Sci.*, *43*, RS4004, doi:10.1029/2007RS003785.

Bilitza, D. (2001), International Reference Ionosphere 2000, *Radio Sci.*, *36*(2), 261–275.

Cabrera, M. A., R. G. Ezquer, and S. M. Radicella (2005), Predicted and measured slant ionospheric electron content, *J. Atmos. Sol. Terr. Phys.*, *67*(16), 1566–1572.

Coïsson, P., S. M. Radicella, R. Leitinger, and B. Nava (2006), Topside electron density in IRI and NeQuick: Features and limitations, *Adv. Space Res.*, *37*, 937–942.

Davies, K., and G. K. Hartmann (1997), Studying the ionosphere with the Global Positioning System, *Radio Sci.*, *32*(4), 1695–1703.

Erturk, O., O. Arikan, and F. Arikan (2009), Tomographic reconstruction of the ionospheric electron density as a function of space and time, *Adv. Space Res.*, *43*, 1702–1710.

EUREF Permanent Network (2013), http://www.epncb.oma.be/_networkdata/stationmaps.php.

Gulyaeva, T. L. (2010), Storm time behavior of topside scale height inferred from the ionosphere-plasmasphere model driven by the F2 layer peak and GPS-TEC observations, *Adv. Space Res.*, *47*(6), 913–920, doi:10.1016/j.asr.2010.10.025.

Gulyaeva, T. L., F. Arikan, and I. Stanislawska (2011), Inter-hemispheric imaging of the ionosphere with the upgraded IRI-Plas model during the space weather storms, *Earth Planets Space*, *63*(8), 929–939, doi:10.5047/eps.2011.04.007.

Gulyaeva, T. L. (2012), Empirical model of ionospheric storm effects on the F_2 layer peak height associated with changes of peak electron density, *J. Geophys. Res.*, *117*, A02302, doi:10.1029/2011JA017158.

Gulyaeva, T. L., and D. Bilitza (2012), Towards ISO Standard Earth Ionosphere and Plasmasphere Model, in *New Developments in the Standard Model*, edited by R. J. Larsen, pp. 1–39, Nova, Hauppauge, New York.

Gulyaeva, T. L., F. Arikan, M. Hernandez-Pajares, and I. Stanislawska (2013), GIM-TEC adaptive ionospheric weather assessment and forecast system, *J. Atmos. Sol. Terr. Phys.*, *102*, 329–340.

Hirooka, S., K. Hattori, M. Nishihashi, S. Kon, and T. Takeda (2012), Development of ionospheric tomography using Neural Network and its application to the 2007 Southern Sumatra earthquake, *Electr. Eng. Jpn.*, *181*(4), 9–18.

International GNSS Service (2013), http://igscb.jpl.nasa.gov/.

Jin, S., and R. Jin (2011), GPS Ionospheric Mapping and Tomography: A case of study in a geomagnetic storm, *IEEE Geoscience and Remote Sensing Symposium (IGARSS) 2011*, 24–29 July 2011, Vancouver, Canada, 1127–1130.

Komjathy, A. (1997), Global ionospheric total electron content mapping using the global positioning system, PhD dissertation, Department of Geodesy and Geomatics Engineering Technical Report No.188, University of New Brunswick, Fredericton, New Brunswick, Canada, 248 pp.

Lanyi, G. E., and T. Roth (1988), A comparison of mapped and measured total ionospheric electron content using Global Positioning System and beacon satellite observations, *Radio Sci.*, *23*(4), 483–492.

Maltseva, O. A., G. A. Zhbankov, and N. S. Mozhaeva (2013), Advantages of the new model of IRI (IRI-Plas) to simulate the ionospheric electron density: Case of the European area, *Adv. Radio Sci.*, *11*, 307–311.

Manucci, A. J., B. D. Wilson, D. N. Yuan, C. H. Ho, U. J. Lindqwister, and T. F. Runge (1998), A global mapping technique for GPS-derived ionospheric total electron content measurements, *Radio Sci.*, *33*, 565–582.

Mushini, S. C., P. T. Jayachandran, R. B. Langley, and J. W. MacDougall (2009), Use of varying shell heights derived from ionosonde data in calculating vertical total electron content (TEC) using GPS—New method, *Adv. Space Res.*, *44*(11), 1309–1313.

Nava, B., P. Coïsson, and S. M. Radicella (2008), A new version of the NeQuick ionosphere electron density model, *J. Atmos. Sol. Terr. Phys.*, *70*(15), 1856–1862.

Nayir, H., F. Arikan, O. Arikan, and C. B. Erol (2007), Total electron content estimation with Reg-Est, *J. Geophys. Res.*, *112*, A11313, doi:10.1029/2007JA012459.

Radicella, S. (2009), The NeQuick model genesis, uses and evolution, *Ann. Geophys.*, *52*(3-4), 417–422.

Schaer, S. (1999), Mapping and predicting the Earth's ionosphere using the Global Positioning System, PhD thesis, Univ. of Bern, Bern, Switzerland.

Sibanda, P. (2010), Challenges in topside ionospheric modelling over South Africa, PhD dissertation, Rhodes University, South Africa.